PHYSICAL REVIEW D **85,** 114001 (2012)

Quark contact interactions at the LHC

F. Bazzocchi,[1,3] U. De Sanctis,[2,3] M. Fabbrichesi,[1] and A. Tonero[1,3]
[1]*INFN, Sezione di Trieste, Trieste, Italy*
[2]*INFN, Gruppo collegato di Udine, Udine, Italy*
[3]*SISSA, via Bonomea 265, 34136 Trieste, Italy*
(Received 22 February 2012; published 1 June 2012)

Quark contact interactions are an important signal of new physics. We introduce a model in which the presence of a symmetry protects these new interactions from giving large corrections in flavor changing processes at low energies. This minimal model provides the basic set of operators which must be considered to contribute to the high-energy processes. To discuss their experimental signature in jet pairs produced in proton-proton collisions, we simplify the number of possible operators down to two. We show (for a representative integrated luminosity of 200 pb^{-1} at $\sqrt{s} = 7$ TeV) how the presence of two operators significantly modifies the bound on the characteristic energy scale of the contact interactions, which is obtained by keeping a single operator.

DOI: 10.1103/PhysRevD.85.114001 PACS numbers: 13.85.Hd, 12.60.Rc, 14.65.Jk

I. MOTIVATIONS

Fermions like quarks can be made to interact directly—that is, without the exchange of an intermediate particle—by simply adding to the standard model (SM) Lagrangian four-quark contact terms like, for example,

$$\frac{2\pi}{\Lambda^2}\,\bar{\psi}_L\gamma^\mu\psi_L\,\bar{\psi}_L\gamma_\mu\psi_L, \tag{1}$$

where 2π gives the strength, Λ is the characteristic energy scale of this new interaction, and the quark fields ψ are taken to be left-handed.

Because of the nonrenormalizability of the term in Eq. (1), such an operator is often thought of as the low-energy effective approximation of a renormalizable Lagrangian in which heavy particles are exchanged. These heavy particles can be of many different kinds, each kind giving rise to an effective operator with different color, flavor, and Dirac structure. Sometimes these heavy states are thought of as a substructure of the quarks themselves and in this case the contact interactions are presented as evidence for quark compositeness. More generally, the heavy states represent new physics, which lives at an energy scale that is too high to manifest itself with the production of the new states either as intermediate resonances or in chain-decay processes, and the effect of which can only be seen by the effective operators of the contact interactions [1]. Nonrenormalizability is not a problem in models in which the couplings run toward an ultraviolet fixed point [2]. In these asymptotically safe models the contact interactions in Eq. (1) can be considered as fundamental. It has recently been shown that indeed such operators arise in a natural manner in asymptotically safe models of the weak interactions, and a search for their presence could provide an important experimental clue [3].

The contact interactions can be fundamental or remnants of new physics; in any case, the search for their existence and the bounds on their characteristic energy scale is important. The LHC has already provided us with new constraints [4–7]. These constraints were derived by assuming the existence of only one kind of contact term, namely that in Eq. (1) in which the operator is given by the product of two left-handed quark currents. This has become the standard practice following [1] because it is simple. Unfortunately, this is too restrictive an assumption and the significance of an analysis based on it is unavoidably weakened.

It is easy to imagine a great variety of different operators contributing to the quark contact interactions. The problem is that this variety is constrained by stringent bounds on flavor physics at low energies [8]. We do not want to track down each and every operator for its possible low-energy effect and, in order to provide a minimal model, we impose a symmetry on the possible contact interactions which makes them safe with respect to these low-energy constraints. This model defines a basic set of operators whose size is not severely constrained by flavor physics and the existence of which can be tested in high-energy processes. It is also general enough to make the bound on the characteristic energy scale Λ realistic.

In principle, all of these operators should be entered in the analysis, each with a different strength. To make the analysis manageable, we further simplify the number of possible operators down to two. This skeleton model is sufficient in showing—in jet pairs produced in proton-proton collisions at the LHC for a representative integrated luminosity of 1 fb^{-1} at $\sqrt{s} = 7$ TeV—how the bound on the energy scale of the contact interactions is sensitive to the relative strengths of different terms. This exercise shows that at least a subset of operators should be taken into account, current analyses based on a single operator cannot be considered as final, and the actual bound

on the characteristic energy scale Λ is weaker than reported [4,6].

II. THE MINIMAL MODEL

Let us for a moment consider the case of a single fermion family with quarks with the same mass. The most general four-quark interaction will depend on the overall symmetry we want to impose on the system. It could be $U(1)_Q$ or $SU(2) \times U(1)$ and in these cases we would have, respectively, 20 or 10 possible terms. Following the general idea that stronger interactions are more symmetric than weaker ones, we want to be more restrictive and impose a larger group $SU(2)_L \times SU(2)_R$ and a parity symmetry.

The complete set of $SU(2)_L \times SU(2)_R$ and parity invariant four-fermion operators is given by four independent terms:

$$\begin{aligned}\mathcal{L}_{\psi^4} = {} & \lambda_1(\bar{\psi}_L^{ia}\psi_R^{ja}\bar{\psi}_R^{jb}\psi_L^{ib}) + \lambda_2(\bar{\psi}_L^{ia}\psi_R^{jb}\bar{\psi}_R^{jb}\psi_L^{ia}) \\ & + \lambda_3(\bar{\psi}_L^{ia}\gamma_\mu\psi_L^{ia}\bar{\psi}_L^{jb}\gamma^\mu\psi_L^{jb} \\ & + \bar{\psi}_R^{ia}\gamma_\mu\psi_R^{ia}\bar{\psi}_R^{jb}\gamma^\mu\psi_R^{jb}) \\ & + \lambda_4(\bar{\psi}_L^{ia}\gamma_\mu\psi_L^{ib}\bar{\psi}_L^{jb}\gamma^\mu\psi_L^{ja} \\ & + \bar{\psi}_R^{ia}\gamma_\mu\psi_R^{ib}\bar{\psi}_R^{jb}\gamma^\mu\psi_R^{ja}), \end{aligned} \tag{2}$$

where the dimensional coefficients λ_n can be written as $2\pi/\Lambda_n^2$ in terms of the characteristic energies Λ_n. Indices i, j and a, b are $SU(2)$ and color indices, respectively.

The operators in Eq. (2) must be considered together with the Yukawa term of the standard model:

$$-\frac{2h}{f}(\bar{\psi}_L^{ia}U^{ij}\psi_R^{ja} + \text{H.c.}). \tag{3}$$

For a realistic model, we should consider the splitting between up- and down-type quarks as well as the three SM families. This gives rise to a large proliferation of possible terms. At the same time, we must take care that the four-fermion operators do not yield unwanted flavor-changing neutral current processes with $\Delta F = 2$, which are strongly suppressed by the experimental data.

In such a realistic and most general case the λ_i in Eq. (2) are 4 flavor-index tensors and the coefficient h in Eq. (3) is a matrix. Thus the four-fermion interaction Lagrangian has 20 4-index tensor operators, that in general are not simultaneously diagonalized with the Yukawa mass terms, thus giving rise to problematic operators such as

$$(\bar{d}_L s_R)^2, \tag{4}$$

which affect, for example, meson oscillations [8].

To prevent such operators and reduce the number of free parameters, one possibility is introducing a flavor symmetry. In the following we assume that left- and right-handed quarks transform as the fundamental representation of a continuous family symmetry we choose to be $SU(3)_F$. In this case the set of four-fermion operators given in Eq. (2) becomes

$$\begin{aligned}\mathcal{L}'_{\psi^4} = {} & \lambda_1(\bar{\psi}_{L_\alpha}^{ia}\psi_{R_\alpha}^{ja}\bar{\psi}_{R_\beta}^{jb}\psi_{L_\beta}^{ib}) + \tilde{\lambda}_1(\bar{\psi}_{L_\alpha}^{ia}\psi_{R_\beta}^{ja}\bar{\psi}_{R_\beta}^{jb}\psi_{L_\alpha}^{ib}) + \lambda_2(\bar{\psi}_{L_\alpha}^{ia}\psi_{R_\alpha}^{jb}\bar{\psi}_{R_\beta}^{jb}\psi_{L_\beta}^{ia}) + \tilde{\lambda}_2(\bar{\psi}_{L_\alpha}^{ia}\psi_{R_\beta}^{jb}\bar{\psi}_{R_\beta}^{jb}\psi_{L_\alpha}^{ia}) \\ & + \lambda_3(\bar{\psi}_{L_\alpha}^{ia}\gamma_\mu\psi_{L_\alpha}^{ia}\bar{\psi}_{L_\beta}^{jb}\gamma^\mu\psi_{L_\beta}^{jb} + \bar{\psi}_{R_\alpha}^{ia}\gamma_\mu\psi_{R_\alpha}^{ia}\bar{\psi}_{R_\beta}^{jb}\gamma^\mu\psi_{R_\beta}^{jb}) + \tilde{\lambda}_3(\bar{\psi}_{L_\alpha}^{ia}\gamma_\mu\psi_{L_\beta}^{ia}\bar{\psi}_{L_\beta}^{jb}\gamma^\mu\psi_{L_\alpha}^{jb} \\ & + \bar{\psi}_{R_\alpha}^{ia}\gamma_\mu\psi_{R_\beta}^{ia}\bar{\psi}_{R_\beta}^{jb}\gamma^\mu\psi_{R_\alpha}^{jb}) + \lambda_4(\bar{\psi}_{L_\alpha}^{ia}\gamma_\mu\psi_{L_\alpha}^{ib}\bar{\psi}_{L_\beta}^{jb}\gamma^\mu\psi_{L_\beta}^{ja} + \bar{\psi}_{R_\alpha}^{ia}\gamma_\mu\psi_{R_\alpha}^{ib}\bar{\psi}_{R_\beta}^{jb}\gamma^\mu\psi_{R_\beta}^{ja}) \\ & + \tilde{\lambda}_4(\bar{\psi}_{L_\alpha}^{ia}\gamma_\mu\psi_{L_\beta}^{ib}\bar{\psi}_{L_\beta}^{jb}\gamma^\mu\psi_{L_\alpha}^{ja} + \bar{\psi}_{R_\alpha}^{ia}\gamma_\mu\psi_{R_\beta}^{ib}\bar{\psi}_{R_\beta}^{jb}\gamma^\mu\psi_{R_\alpha}^{ja}), \end{aligned} \tag{5}$$

where α, β are $SU(3)_F$ flavor indices. The symmetry of the four-fermion interactions is thus $SU(2)_L \times SU(2)_R \times SU(3)_F$.

In this minimal model there are 8 arbitrary coefficients—the λ_n and $\tilde{\lambda}_n$ in Eq. (5)—each of them multiplying various operators which are different for flavor and color structure. In a numerical study, all coefficients should, in principle, be varied and the most relevant among the operators included.

For what concerns the Yukawa term given in Eq. (3), first of all we have to split up- and down-type quarks:

$$\begin{aligned} & -\frac{2h^u_{\alpha\beta}}{f}(\bar{\psi}_{L_\alpha}^{ia}U^{ij}P_u\psi_{R_\beta}^{ja} + \text{H.c.}) \\ & -\frac{2h^d_{\alpha\beta}}{f}(\bar{\psi}_{L_\alpha}^{ia}U^{ij}P_d\psi_{R_\beta}^{ja} + \text{H.c.}), \end{aligned} \tag{6}$$

where the projectors $P_{u,d}$ project on the up and down components of ψ_R^{ja}, respectively.

In the most general case Eq. (6) breaks the full group $SU(2)_L \times SU(2)_R \times SU(3)_F$ to the electric charge $U(1)_Q$ in a completely arbitrary way. However, if we think of the $h^{u,d}_{\alpha\beta}$ as arising from the vacuum expectation values of a field Y, they can be written as $h^{u,d} = \langle Y^{u,d}\rangle/\Lambda_F$ and, in this case, the Yukawa Lagrangian that leads to Eq. (6) presents the extra accidental global symmetry $SU(3)^Q_{F_L} \times SU(3)^u_{F_R} \times SU(3)^d_{F_R}$ according to which $Y^{u,d}$ transform as the $(3, \bar{3}, 1)$ and $(3, 1, \bar{3})$ representations, respectively. We may now assume that $Y^{u,d}$ develops the vacuum expectation value only along the diagonal direction $SU(3)^u_{F_V} \times SU(3)^d_{F_V}$: in this way, the Yukawa mass matrices $h^q (q = u, d)$ are symmetric and $V_L^q = V_R^q$. Notice that

$V_L^{u,d}$ satisfy $V_{\rm CKM} = V_L^{u\dagger} V_L^d$, and, thanks to our assumptions, $V_{\rm CKM} = V_R^{u\dagger} V_R^d$. Thus in the Yukawa sector the full symmetry $SU(3)^Q_{F_L} \times SU(3)^u_{F_R} \times SU(3)^d_{F_R} \supset SU(3)^u_{F_V} \times SU(3)^d_{F_V}$ is broken to $[U(1)^u]^3_F \times [U(1)^d]^3_F$.

It is now simple to identify whether a term of the four-fermion operators of Eq. (5) may give rise to flavor violation or not: those terms that are invariant under $SU(3)^u_{F_V} \times SU(3)^d_{F_V}$ do not violate flavor because they are simultaneously diagonalized with the Yukawa couplings; the others do.

Indeed, if we classify quarks according to their electric charge q and their flavor charge q_F, we see that when in the four-fermion operators flavor indices are contracted between quarks of the same electric charge q automatically, the total q_F is zero for each flavor involved. This happens for exactly 14 operators (each with 2 indices running over the 3 families):

(i) 2 operators from $\lambda_1(\lambda_2)$ and 4 operators from $\tilde\lambda_1(\tilde\lambda_2)$, 2 of which have the same structure of those from $\lambda_1(\lambda_2)$, for a total of 8 operators;
(ii) 2 operators from $\tilde\lambda_3(\tilde\lambda_4)$ and 3 operators from $\lambda_3(\lambda_4)$, 2 of which have the same structure of those from $\tilde\lambda_3(\tilde\lambda_4)$, for a total of 6 operators.

These operators correspond to a subset of possible contractions and give rise to the Lagrangian

$$\begin{aligned}\mathcal{L}^{(0)}_{\psi^4} = {} & (\lambda_1+\tilde\lambda_1)[\bar u^a_{L_A} u^a_{R_A} \bar u^b_{R_B} u^b_{L_B} + \bar d^a_{L_A} d^a_{R_A} \bar d^b_{R_B} d^b_{L_B}] + \tilde\lambda_1[\bar u^a_{L_A} d^a_{R_B} \bar d^b_{R_A} u^b_{L_B} + \bar d^a_{L_A} u^a_{R_B} \bar u^b_{R_A} d^b_{L_B}] + \lambda_3 \bar u^a_{L_A} \gamma_\mu u^a_{L_A} \bar d^b_{L_B} \gamma^\mu d^b_{L_B} \\ & + (\lambda_3+\tilde\lambda_3)[\bar u^a_{L_A} \gamma_\mu u^a_{L_A} \bar u^b_{L_B} \gamma^\mu u^b_{L_B} + \bar d^a_{L_A} \gamma_\mu d^a_{L_A} \bar d^b_{L_B} \gamma^\mu d^b_{L_B}] + (\lambda_2+\tilde\lambda_2)[\bar u^a_{L_A} u^b_{R_A} \bar u^b_{R_B} u^a_{L_B} + \bar d^a_{L_A} d^b_{R_A} \bar d^b_{R_B} d^a_{L_B}] \\ & + \tilde\lambda_2[\bar u^a_{L_A} d^b_{R_B} \bar d^b_{R_A} u^a_{L_B} + \bar d^a_{L_A} u^b_{R_B} \bar u^b_{R_A} d^a_{L_B}] + \lambda_4 \bar u^a_{L_A} \gamma_\mu u^b_{L_A} \bar d^b_{L_B} \gamma^\mu d^a_{L_B} + (\lambda_4+\tilde\lambda_4)[\bar u^a_{L_A} \gamma_\mu u^b_{L_A} \bar u^b_{L_B} \gamma^\mu u^a_{L_B} \\ & + \bar d^a_{L_A} \gamma_\mu d^b_{L_A} \bar d^b_{L_B} \gamma^\mu d^a_{L_B}], \end{aligned} \tag{7}$$

where A, B are mass eigenstates indices, while a, b are color indices (notice the different color contractions in the various similar operators). This Lagrangian has, as before in Eq. (5), 8 coefficients and 14 operators. Each of these operators generates 6 terms once the 3 families are included.

On the contrary, when flavor indices are contracted between quarks that have $|\Delta q| = 1$ the operators present a total $q_F \neq 0$. This is the case for 6 operators:

(i) 2 operators from $\lambda_1(\lambda_2)$, for a total of 4 operators;
(ii) 1 operator from $\tilde\lambda_3(\tilde\lambda_4)$ for a total of 2 operators.

The corresponding operators become 4 flavor-index tensors, the structure dictated by the $V_{\rm CKM}$ entries according to

$$\begin{aligned}\mathcal{L}^{(1)}_{\psi^4} = {} & \lambda_1[(V_{\rm CKM})_{AB}(V^\dagger_{\rm CKM})_{CD}(\bar u^a_{L_A} d^a_{R_B})(\bar d^b_{R_C} u^b_{R_D}) + (V^\dagger_{\rm CKM})_{AB}(V_{\rm CKM})_{CD}(\bar d^a_{L_A} u^a_{R_B})(\bar u^b_{R_C} d^b_{R_D})] \\ & + \tilde\lambda_3 (V_{\rm CKM})_{AD}(V^\dagger_{\rm CKM})_{BC}(\bar u^a_{L_A} \gamma_\mu u^a_{L_B})(\bar d^b_{L_C} \gamma^\mu d^b_{L_D}) + \lambda_2[(V_{\rm CKM})_{AB}(V^\dagger_{\rm CKM})_{CD}(\bar u^a_{L_A} d^b_{R_B})(\bar d^b_{R_C} u^a_{R_D}) \\ & + (V^\dagger_{\rm CKM})_{AB}(V_{\rm CKM})_{CD}(\bar d^a_{L_A} u^b_{R_B})(\bar u^b_{R_C} d^a_{R_D})] + \tilde\lambda_4 (V_{\rm CKM})_{AD}(V^\dagger_{\rm CKM})_{BC}(\bar u^a_{L_A} \gamma_\mu u^b_{L_B})(\bar d^b_{L_C} \gamma^\mu d^a_{L_D}). \end{aligned} \tag{8}$$

For the operators in Eq. (8), flavor breaking is manifest since they are characterized by $q_X = \pm 1$ with $X = A, B, C, D$. However, these operators may mediate flavor-changing neutral current $\Delta F = 2$ processes only at one loop. Thanks to the suppression related to the entries of the Cabibbo-Kobayashi-Maskawa (CKM) matrix, their effect is of the same order, or even smaller, than the SM contributions.

To summarize: by imposing an appropriate flavor symmetry, the large number of four-fermion operators present in the most general case have been grouped in two classes: one that includes operators that conserve flavor, the other which includes those that violate it. These operators multiply different combinations of the 8 independent parameters λ_n and $\tilde\lambda_n$ in Eq. (5). Flavor violating operators are modulated by the square of CKM entries and are therefore suppressed. When considering pp collisions, the flavor-conserving operators in Eq. (7) dominate on those in Eq. (8)—which as a consequence can be neglected. Moreover, among the operators in Eq. (7), the largest cross sections are given by those involving only the first family in the initial state and the first, and possibly the second, family in the final state. Therefore, a complete analysis of this minimal model should take into account at least the 14 operators in the Lagrangian $\mathcal{L}^{(0)}_{\psi^4}$ of Eq. (7) involving the first family to set bounds on the 8 parameters λ_n and $\tilde\lambda_n$.

III. EVENT GENERATION AND ANALYSIS OF THE SKELETON MODEL

Dijet production in proton-proton collisions $pp \to jj + X$ is the best channel to search for quark contact interactions. In QCD, the jet production rate peaks at large

rapidity y, because the scattering is dominated by t-channel processes. The rapidity is defined as $y = \frac{1}{2}\ln(E + p_z)/(E - p_z)$, where E is the energy and p_z is the z component of momentum of a given particle. On the other hand, quark contact interactions produce a more isotropic angular distribution leading to enhanced jet production at smaller values of $|y|$. For this reason, searches for contact interactions at the LHC use quantities computed from these dijet rapidity distributions in the high invariant dijet mass (m_{jj}) region.

In current analyses [4,6], the contact interactions are parametrized by a single standard operator, the one introduced in [1]—where, however, a larger set of operators was introduced and the single-operator scenario was only advocated as a simplification. As we argued in the previous section, a standard set of operators can be identified. The simulation of the 14 operators and 8 parameters is rather CPU time consuming and here we only consider the effect of the presence of more than one operator on dijet production by introducing a skeleton model that admits just two four-fermion operators, which we chose to be the first and the third of Eq. (2). The size of their couplings are parametrized by the characteristic energy scales Λ_1 and Λ_3. While a full analysis is certainly necessary, such a radical simplification is already sufficient in showing how the presence of more than one operator gives rise to substantial interference effects which modify the bounds on the characteristic energy scale.

The Lagrangian of this skeleton model, written in terms of these parameters, reads

$$\mathcal{L} = \mathcal{L}_{\mathrm{QCD}} + \frac{2\pi}{\Lambda_3^2}(\bar{\psi}_L\gamma_\mu\psi_L\bar{\psi}_L\gamma^\mu\psi_L + \bar{\psi}_R\gamma_\mu\psi_R\bar{\psi}_R\gamma^\mu\psi_R) + \frac{2\pi}{\Lambda_1^2}(\bar{\psi}_L\psi_R\bar{\psi}_R\psi_L), \quad (9)$$

where the isospin and the color contractions, that can be read out directly from Eq. (2), are omitted.

This choice of considering just two operators is useful because it reduces the CPU time for the simulation, simplifies the analysis, and shows how it is essential to consider more than one operator.

We use MADGRAPH/MADEVENT V.4.5.0 [9] to simulate LHC dijet production in pp collisions at $\sqrt{s} = 7$ TeV; Monte Carlo samples are generated for pure QCD and for QCD modified by the new four-fermion interaction terms in Eq. (9). Since MADGRAPH is a leading-order generator and does not support nonrenormalizable interactions, we have implemented them effectively, introducing a set of fictitious gauge interactions acting only on the first quark family. In this case, the identification is $\psi = (ud)$, and the mass of the fictitious gauge boson has been chosen to be very high (~ 100 TeV). Hadronization and showering are implemented by PYTHIA V6.4 [10], which is included in MADEVENT. Then the generated events are then passed through PGS [11], the detector simulator in which the parameters are set to reproduce the ATLAS detector performance.

In order to restrict the simulation in the kinematical region of interest, we have applied the following cuts at the generator level:

(i) $m_{jj} > 1000$ GeV;
(ii) $p_T^{j_1}, p_T^{j_2} > 30$ GeV;
(iii) $|\eta^{\mathrm{jet}}| < 2.8$.

The pseudorapidity is defined as $\eta = -\ln(\tan\theta/2)$, where θ is the angle between the jet and the beam direction in the laboratory frame.

We have generated Monte Carlo samples for different values of the energy scales Λ_1 and Λ_3 between 1 and 10 TeV.

Given the cuts described above, the Monte Carlo leading order cross section for each choice of the parameters turns out to be $\sigma \simeq 5 \times 10^3$ pb. An integrated luminosity of 1 fb^{-1} has been generated for each of the points in the (Λ_1, Λ_3) plane described above.

The variable χ is the quantity used for the angular distribution study. It is defined as a function of the rapidities of the two highest p_T jets in the event, y_1 and y_2:

$$\chi = \exp(2|y^*|). \quad (10)$$

In the massless particle limit the center-of-mass (CM) rapidity $y^* = (y_1 - y_2)/2$ is used to determine the partonic CM angle θ^* given the relation $y^* = \frac{1}{2}\ln(\frac{1+|\cos\theta^*|}{1-|\cos\theta^*|})$.

The dominant subprocesses for dijet production at LHC are $gu \to gu$, $gg \to gg$, and $uu \to uu$. For each of these, the θ^* distributions have the familiar Rutherford behavior, which is characteristic of massless vector exchange in the t channel. To study deviations from this behavior, it is convenient to plot distributions in terms of the variable χ, which removes the Rutherford singularity.

In terms of this variable, the dijet $dN/d\chi$ distribution obtained from the leading QCD subprocesses is almost flat. This angular distribution is slightly modified also considering the other subdominant processes, which include gluon exchange in the s channel, that can rise the distribution at low χ and taking into account next-to-leading QCD predictions [12] which lead to an increasing of the number of events at high χ [13]. On the other hand, in the case of new physics processes, which are more isotropic, the total dijet angular distribution can be considerable modified by the presence of additional events in the low χ region, as shown in Fig. 1. The second important kinematic variable is the dijet invariant mass m_{jj}, which is also the CM energy of the partonic system. It is computed from the two jet four-vectors as

$$m_{jj} = \sqrt{(E^{j1} + E^{j2})^2 - (\mathbf{p}^{j1} + \mathbf{p}^{j2})^2}, \quad (11)$$

where E and $\mathbf{p}$ are the energy and momentum of the jets.

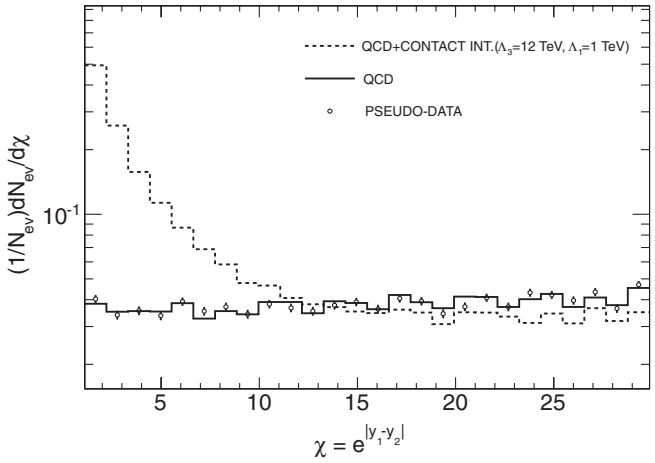

FIG. 1. χ distribution, as defined in Eq. (10) for events with $m_{jj} \geq 1200$ GeV. Empty points represent the χ distribution for pseudodata, the solid line for pure QCD, while the dotted line for one specific point ($\Lambda_1 = 1$ TeV, $\Lambda_3 = 12$ TeV) in the generated grid. The various distributions are normalized to an integrated luminosity of 200 pb^{-1}.

Events with at least two jets are retained if the highest p_T jet satisfies $p_T^{j1} > 60$ GeV and the second highest one satisfies $p_T^{j2} > 30$ GeV. This asymmetric threshold avoids suppression of events where a third jet has been radiated, while the 30 GeV threshold ensures that reconstruction is fully efficient for both leading jets. Events with an additional poorly measured jet with $p_T > 15$ GeV are vetoed to avoid possible incorrect identification of the two leading jets. Another variable useful to cut the data, derived from the rapidities of the two jets, is $y_B = (y_1 + y_2)/2$. Distributions are accumulated only for events for which $|y_B| < 1.10$ and $|y^*| < 1.70$. This is done in order to be consistent with the analysis in [6].

The measure of the isotropy in the dijet distribution, introduced in [6], is given by the variable F_χ. It measures the fraction of dijets produced centrally versus the total number of observed dijets in a specified dijet mass range:

$$F_\chi = \frac{N_{\text{events}}(|y^*| < 0.6)}{N_{\text{events}}(|y^*| < 1.7)}, \tag{12}$$

where N_{events} is the number of candidate events within the y^* interval. The central region which is expected to be most sensitive to new physics is defined by the interval $|y^*| < 0.6$ and corresponds to $\chi < 3.32$, while $|y^*| < 1.7$ extends the angular range to $\chi < 30$.

The presence of possible contact terms is tested for each value of Λ_1 and Λ_3 in the highest dijet mass bin: $m_{jj} \geq 1200$ GeV. For a given pair of values of the energy scales, the corresponding value of F_χ is obtained starting from the χ distribution as in Fig. 1. We have generated a QCD Monte Carlo sample, corresponding to an integrated luminosity of 200 pb^{-1}, to be used as a pseudodata sample. In Fig. 1, the χ distribution is shown for dijet events passing the selection described above with the additional constraint that the invariant mass of the two hardest jets is larger than 1200 GeV. The pseudodata sample (empty points) is well described by the QCD (solid line), while the contribution of a contact interaction term (dotted line), corresponding to the point ($\Lambda_1 = 1$ TeV, $\Lambda_3 = 12$ TeV) in the grid, clearly shows a peak in the low χ region, giving then a larger values for F_χ [defined in Eq. (12)] with respect to both pseudodata and QCD samples. A full set of pseudoexperiments has then been made for each of the points in the grid in order to construct one-sided 95% confidence level.

The result of this analysis is shown by the contour plot of Fig. 3. The value of F_χ extracted from the pseudodata represents in Fig. 2 the level below which the contact

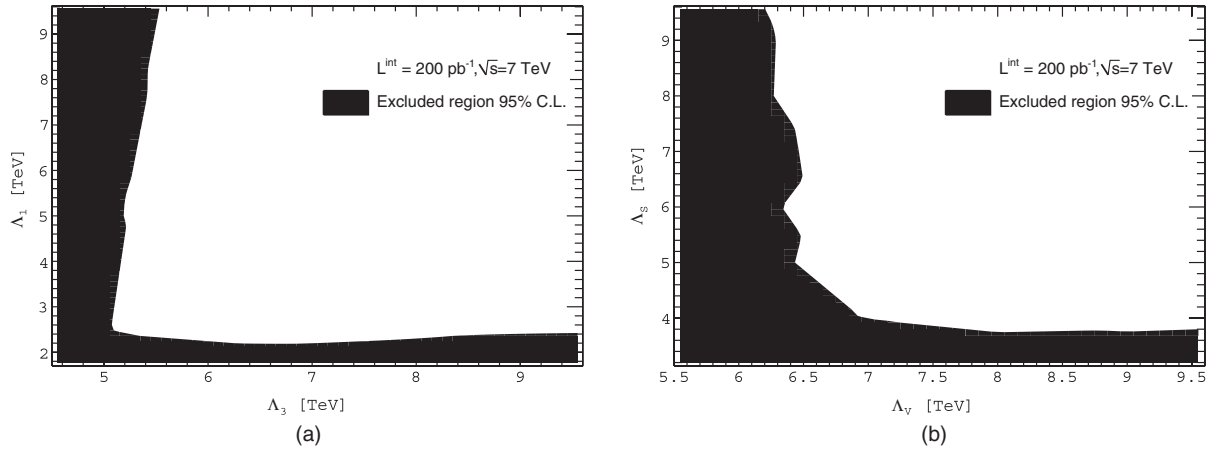

FIG. 2. F_χ 95% confidence level contour plot. The area inside the curve represents—at the 95% confidence level—values of F_χ, obtained for different values of the energy scales Λ's, compatible with the pseudodata measured quantity. Figure 2(a) is the 95% confidence level plot for the F_χ variable measured for different values of Λ_1 and Λ_3 (see text). The lower bounds for Λ_1 and Λ_3 are, respectively, 2.2 and 5.1 TeV. Figure 2(b) is the 95% confidence level plot for the F_χ variable measured for different values of the common scales Λ_S and Λ_V (see text). The lower bounds for Λ_S and Λ_V are, respectively, 3.9 and 6.3 TeV.

interactions are compatible with pseudodata. The values of Λ_1 and Λ_3 which satisfy—at the 95% confidence level—this bound are represented by the area inside the curve. By inspection, we find that the lower bounds on the contact interaction scale are given by the values $\Lambda_1 = 2.2$ TeV and $\Lambda_3 = 5.1$ TeV, respectively.

The standard one-operator analysis—which corresponds to taking Λ_1 very large—would give a limit of $\Lambda_3 = \Lambda \approx 5.6$ TeV which corresponds to the upper margin of the not excluded area in the contour plot in Fig. 3. The bounds we find in the case of two operators are weaker than this one because of interference effects.

For comparison, in Fig. 3 we show the result when we switch on all four operators of Eq. (2). We assume two common interaction scales Λ_S and Λ_V for the scalar and vector type operators, respectively. This choice corresponds to setting $\lambda_1 = \lambda_2 = 2\pi/\Lambda_S^2$ and $\lambda_3 = \lambda_4 = 2\pi/\Lambda_V^2$. We therefore have again just two operators. By inspection, we find that the lower bounds on these common contact interaction scales are given by the values $\Lambda_S = 3.9$ TeV and $\Lambda_V = 6.3$ TeV.

If one insists in having a unique energy scale Λ even in the presence of more operators, it possible to provide it by combining the characteristic scales Λ_n by means of, for instance, the definition

$$\frac{1}{\Lambda^2} = \sum_{n=1}^{8} \frac{1}{\Lambda_n^2}. \tag{13}$$

This definition has the advantage of providing a bound close to the lowest one and to go into the single-operator limit when all scales but one are taken to be large. In our skeleton model with just two scales Λ_1 and Λ_2, the definition in Eq. (13) gives a bound $\Lambda = 2.0$ TeV—a value again weaker than what found in the single-operator analysis.

ACKNOWLEDGMENTS

We thank O. Mattelaer and C. Degrande for help with MADGRAPH. We thank G. Choudalakis, F. Ruehr, and F. Meloni for their helpful suggestions in performing the analysis.

[1] E. Eichten, K. D. Lane, and M. E. Peskin, Phys. Rev. Lett. **50**, 811 (1983); E. Eichten, I. Hinchliffe, K. D. Lane, and C. Quigg, Rev. Mod. Phys. **56**, 579 (1984); R. S. Chivukula and H. Georgi, Phys. Lett. B **188**, 99 (1987); E. N. Argyres, G. A. Katsilieris, C. G. Papadopoulos, and S. D. P. Vlassopulos, Int. J. Mod. Phys. A **7**, 7915 (1992); A. A. Babich, G. Della Ricca, J. Holt, P. Osland, A. A. Pankov, and N. Paver, Eur. Phys. J. C **29**, 103 (2003); C. Degrande, J.-M. Gerard, C. Grojean, F. Maltoni, and G. Servant, J. High Energy Phys. 03 (2011) 125.

[2] S. Weinberg, in *General Relativity: An Einstein Centenary Survey*, edited by S. W. Hawking and W. Israel (Cambridge University Press, Cambridge, England, 1979), pp. 790–831; M. Niedermaier and M. Reuter, Living Rev. Relativity **9**, 5 (2006); R. Percacci, in *Approaches to Quantum Gravity: Towards a New Understanding of Space, Time and Matter*, edited by D. Oriti (Cambridge University Press, Cambridge, England, 2009).

[3] F. Bazzocchi, M. Fabbrichesi, R. Percacci, A. Tonero, and L. Vecchi, Phys. Lett. B **705**, 388 (2011).

[4] V. Khachatryan *et al.* (CMS Collaboration), Phys. Rev. Lett. **106**, 201804 (2011).

[5] CMS Collaboration, Report No. CERN-PH-EP/2012-044.

[6] G. Aad *et al.* (ATLAS Collaboration), Phys. Lett. B **694**, 327 (2011); New J. Phys. **13**, 053044 (2011).

[7] ATLAS Collaboration, Report No. ATLAS-CONF-2012-038, 2012.

[8] M. Bona *et al.* (UTfit Collaboration), J. High Energy Phys. 03 (2008) 049.

[9] MADGRAPH/MADEVENT V4, in J. Alwall, P. Demin, S. de Visscher, R. Frederix, M. Herquet, F. Maltoni, T. Plehn, D. L. Rainwater, and T. Stelzer, J. High Energy Phys. 09 (2007) 028.

[10] PYTHIA 6.4, in T. Sjostrand, S. Mrenna, and P. Skands, J. High Energy Phys. 05 (2006) 026.

[11] M. Carena *et al.* (Higgs Working Group Collaboration), in *Physics at Run II: The Supersymmetry/Higgs Workshop, Fermilab, 1998*, edited by M. Carena and J. Lykken (Fermilab, Batavia, 2002), p. 424.

[12] S. D. Ellis, Z. Kunszt, and D. E. Soper, Phys. Rev. Lett. **69**, 3615 (1992).

[13] G. C. Blazey (D0 Collaboration), Proceeding of the 31st Recontres de Moriond:QCD and High-Energy Hadronic Interactions, Les Arcs, France, Report No. Fermilab-Conf-96-132-E, 1986.